# Passivity-Based Integral Sliding Mode Control for Robust Trajectory Tracking in 2-DOF Helicopter Systems

Ratiba FELLAG[(1)*], Mahmoud BELHOCINE[(1)], Meziane HAMEL[(2)]
[(1)] Robotics and Industrial Automation Laboratory, Centre de Développement des Technologies Avancées (CDTA), Algiers, Algeria
[(2)] Laboratory of Energy and Mechanical Engineering (LEMI), M'Hamed Bougara University, Boumerdès, Algeria
[*]rfellag@cdta.dz

**Abstract:** This study introduces a robust trajectory-tracking control strategy in a two-degrees-of-freedom (2-DOF) helicopter system, combining passivity theory and integral sliding mode control (ISMC) strengths. The proposed integral passivity-based sliding mode control (IPBSMC) integrates passivity-based energy shaping, which inherently accounts for the system's natural dynamics, with integral sliding mode control to enhance tracking performance and reduce control effort. The controller's effectiveness is validated through simulations and real-time experiments with band-limited white noise disturbances using the Quanser AERO 2 platform interfaced with MATLAB/Simulink. Results indicate good trajectory tracking, with steady-state errors below ±0.2 rad under non-vanishing Gaussian disturbances. The experimental implementation further validates the proposed method's practical applicability and highlights its potential for real-world deployment in coupled systems requiring high accuracy and robustness under varied operating conditions.

**Keywords:** Integral Sliding Mode Control, Passivity-Based Control, 2-DOF Helicopter, Robust Control, Trajectory Tracking

## 1. INTRODUCTION

The control of rotary-wing unmanned aerial vehicles (UAVs) has evolved into a critical research domain within robotics and control communities, driven by their expanding applications in surveillance, transportation, precision agriculture, and aerial manipulation [1-3]. Helicopter-type UAVs, with their vertical take-off and landing capabilities and hovering ability, represent one of the most versatile configurations in this class of vehicles. A prominent example in control research is the Quanser Aero 2, a two-degree-of-freedom (2-DOF) helicopter system that serves as a fundamental yet challenging testbed for developing and validating advanced control methodologies. This platform is particularly well-suited for studying systems characterized by significant cross-coupling effects, inherent nonlinearities, and susceptibility to external disturbances [4, 5].

Traditional control approaches such as PID and LQR have shown significant limitations when applied to such complex nonlinear systems, particularly under uncertainty and disturbance conditions [6]. This shortcoming has motivated extensive research into robust nonlinear control techniques capable of addressing these challenges.

Among these, Sliding Mode Control (SMC) stands out due to its inherent robustness against disturbances and parameter variations [7, 8]. However, conventional SMC suffers from two key drawbacks: high-frequency chattering, which can excite unmodeled dynamics, and excessive control effort [9, 10]. Integral Sliding Mode Control (ISMC) has been developed to overcome these issues while preserving robustness. Unlike conventional SMC, ISMC eliminates the reaching phase by designing the sliding variable such that the system starts directly on the sliding surface from the initial time instant [11, 12]. As a result, ISMC ensures global

robustness, including during the transient response.

Concurrently, Passivity-Based Control (PBC) exploits the system's natural energy properties to achieve desired control objectives while guaranteeing closed-loop stability [13, 14]. By framing the control problem in terms of energy exchange and dissipation, PBC yields controllers that align with the system's physical structure [15]. This energy-based perspective also provides a natural Lyapunov function candidate, simplifying stability analysis and offering intuitive physical interpretability [13, 16]. However, PBC's effectiveness relies heavily on accurate system modeling, motivating integration with robust control techniques to address modeling uncertainties and external disturbances [17, 18].

This paper presents a hybrid Passivity-Based Integral Sliding Mode Control (IPBSMC) scheme for the Quanser AERO 2 platform, combining the strengths of PBC and ISMC to address their individual limitations. The proposed integration achieves four key advantages: (1) retention of PBC's physically interpretable stability framework while incorporating ISMC's disturbance robustness, (2) enhanced transient performance through integral sliding mode dynamics while preserving energy-based system shaping, (3) natural chattering reduction via passivity-based damping injection without compromising rejection capabilities, and (4) minimized control effort by utilizing PBC for nominal dynamics, reducing traditional SMC high-gain requirements. Comprehensive validation through simulation and real-time implementation on the Quanser AERO 2 platform confirms practical effectiveness under band-limited white noise disturbances, demonstrating superior performance metrics and establishing foundation for energy-efficient robust control of complex nonlinear systems.

## 2. SYSTEM DESCRIPTION AND MODELING

The experimental setup used in this work is Quanser's Aero 2 platform [4], depicted in Fig. 1. It features a pivoting arm attached to a stationary frame with two thrusters powered by DC motors. For precise attitude control, the apparatus is equipped with an IMU (Inertial Measurement Unit) and four optical encoders, all interfaced with a real-time data acquisition


Fig. 1 Quanser Aero 2 platform [4].

system to regulate pitch and yaw dynamics [11].

Using Euler-Lagrange formalism, the nonlinear dynamic model of the Quanser Aero 2 is expressed as:

$$M(q)\ddot{q}+C(q,\dot{q})\dot{q}+F\dot{q}+G(q)=\tau \quad (1)$$

Where $M$ is the inertia matrix, $C$ is the centrifugal forces matrix, $F$ is the viscous damping, G is the gravity, and $\tau$ is the applied torques. Accordingly, $\theta$ with representing the pitch angle and $\psi$ the yaw angle, we have:

$$q=\begin{bmatrix}\theta & \psi\end{bmatrix}^T, u=\begin{bmatrix}V_p & V_y\end{bmatrix}^T, \Lambda=\begin{bmatrix}K_{pp} & K_{py}\\ K_{yp} & K_{yy}\end{bmatrix} \quad (2)$$

$$M(q)=\begin{bmatrix}J_p+m_h l_{cm}^2 & 0\\ 0 & J_h+m_h l_{cm}^2\cos\theta^2\end{bmatrix} \quad (3)$$

$$C(q,\dot{q})=\begin{bmatrix}0 & m_h l_{cm}^2\sin\theta\cos\theta\dot{\psi}\\ -2m_h l_{cm}^2\sin\theta\cos\theta\dot{\psi} & 0\end{bmatrix} \quad (4)$$

$$F=\begin{bmatrix}F_p & 0\\ 0 & F_y\end{bmatrix} \quad (5)$$

$$G(q)=\begin{bmatrix}m_h g l_{cm}\cos\theta\\ 0\end{bmatrix} \quad (6)$$

$$\tau=\Lambda\,\mathrm{u} \quad (7)$$

The different parameters of the dynamic model are given in the following Table. 1. [5]

**Table 1.** Dynamic parameters of the Aero 2 [5].

| Symbol | Description | Value |
|---|---|---|
| $J_p$ | Pitch axis inertia | 0.0232 $Kg.m^2$ |
| $J_y$ | Yaw axis inertia | 0.0238 $Kg.m^2$ |
| $F_p$ | Pitch axis damping | 0.0020 $N.m/V$ |
| $F_y$ | Yaw axis damping | 0.0019 $N.m/V$ |
| $K_{pp}$ | Pitch thrust gain from front rotor | 0.0032 $N/V$ |
| $K_{py}$ | Pitch thrust gain from rear rotor | 0.0014 $N/V$ |
| $K_{yy}$ | Yaw thrust gain from rear rotor | 0.0061 $N/V$ |
| $K_{yp}$ | Yaw thrust gain from front rotor | -0.0032 $N/V$ |
| $l_{cm}$ | Distance between pivot and rotor | 0.1674 $m$ |
| $m_h$ | Helicopter mass | 4.7kg |
| $g$ | Gravity | 9.81m/s$^2$ |

## 3. CONTROLLER DESIGN

The control objective centers on achieving asymptotic tracking performance, where the error vector $e = q - q_d$ converges to zero despite persistent disturbances. The IPBSMC strategy accomplishes this through the strategic integration of energy-based dynamics shaping with robust sliding mode control.

The dynamic equation (1) with tracking error becomes:

$$M(q)(\ddot{e}+\ddot{q}_d)+C(q,\dot{q})(\dot{e}+\dot{q}_d)+F(\dot{e}+\dot{q}_d)+\ldots \\ G(q)=\tau \quad (8)$$

By rearranging the terms, we get:

$$M(q)\ddot{e}+C(q,\dot{q})\dot{e}+F\dot{e}=\tau-G(q)-M(q)\ddot{q}_d \\ -C(q,\dot{q})\dot{q}_d-F\dot{q}_d \quad (9)$$

We select the integral sliding surface as:

$$s = \dot{e}+\lambda e+\lambda_i\int_0^t e\,dt \quad (10)$$

With

$$\lambda = diag(\lambda_\theta,\lambda_\psi) \quad (11)$$

$$\lambda_i = diag(\lambda_{i\theta},\lambda_{i\psi}) \quad (12)$$

$\lambda_\theta,\lambda_\psi$ and $\lambda_{i\theta},\lambda_{i\psi}$ are positive gains of the sliding surface for the pitch and yaw axes.

The integral sliding surface (10) is designed to eliminate the reaching phase inherent in conventional SMC, ensuring robustness from the initial time. The integral term provides additional design freedom for transient response shaping while maintaining steady-state accuracy.

The sliding mode characteristic of the passivity-based control system is achieved by maintaining the integral sliding surface (10) at zero. For this control strategy, the following storage function candidate has been selected:

$$V = \frac{1}{2}s^{\mathrm{T}}Ms \quad (13)$$

Equation (13) is positive definite, and by incorporating equations (9) and (10), its time derivative can be computed as:

$$\dot{V} = s^{\mathrm{T}}M\dot{s}+\frac{1}{2}s^{\mathrm{T}}\dot{M}s \quad (14)$$

$$\dot{V} = s^{\mathrm{T}}\begin{pmatrix}\tau-G(q)-M\ddot{q}_d-C\dot{q}_d-F\dot{q}_d-C\dot{q}_e-\ldots \\ F\dot{e}+M\lambda\dot{e}+M\lambda_i e+\frac{1}{2}\dot{M}s\end{pmatrix} \quad (15)$$

$$\dot{V} = s^{\mathrm{T}}\begin{pmatrix}\tau-G(q)-(F+C)\dot{q}+M(\lambda\dot{e}+\lambda_i e-\ddot{q}_d)+\ldots \\ \frac{1}{2}\dot{M}s\end{pmatrix} \quad (16)$$

At this step, we choose the control as:

$$\tau = G(q)+(F+C)\dot{q}-M(\lambda\dot{e}+\lambda_i e-\ddot{q}_d)- \\ \frac{1}{2}\dot{M}s+v \quad (17)$$

The robustness term $v$ is selected as (18).

$$v = -\gamma sign(s) \quad (18)$$

In practical implementation, the sign function is replaced by the function $\tanh(s)$ to mitigate chattering. It provides a continuous approximation to ideal switching while maintaining the essential robustness properties. γ is a positive gain vector.

$$v = -\gamma\tanh(s) \quad (19)$$

Replacing (17) and (19) in (16), we obtain:

$$\dot{V} = -s^T(\gamma\tanh(s)) \quad \leq 0 \quad (20)$$

Which satisfies the following inequalities of being a passive system with the output $y = s$ and $v = -\varphi(y)$.

$$v^T y \geq \dot{V} \quad (21)$$

This condition (21) signifies that the system from input *v* to output *s* is lossless, a specific case of passivity.

$$y^T\varphi(y) > 0, \quad \forall y \neq 0 \quad (22)$$

With $s^T(\gamma\tanh(s)) = \sum_i \gamma_i s_i \tanh(s_i)$. Since $\gamma_i > 0$ and $x\tanh(x) > 0$ for $x \neq 0$, then condition (22) is satisfied.

$$\varphi(0) = 0 \quad (23)$$

Condition (23) is correctly satisfied, since $\varphi(0) = \gamma\tanh(0) = 0$.

Furthermore, when $v = 0$,

$$y \equiv 0 \Rightarrow s \equiv 0 \quad (24)$$

Given $v = -\gamma\tanh(s)$, $v = 0$ implies $-\gamma\tanh(s) = 0$. Since $\gamma_i > 0$, this means $\tanh(s_i) = 0$, so $s_i = 0$, and thus $s = 0$, condition (24) satisfied. Using LaSalle's Invariance Principle with $\dot{V} = -s^T(\gamma\tanh(s))$, the largest invariant set where $\dot{V} = 0$ is $s = 0$. This implies s→0. The stability of the sliding surface dynamics ($s = \dot{e}+\lambda e+\lambda_i\int e\,dt$) then ensures e→0.

Finally, the overall control signal is obtained as

$$u = \Lambda^{-1}\begin{pmatrix}G(q)+(F+C)\dot{q}-M(\lambda\dot{e}+\lambda_i e-\ddot{q}_d)- \\ \frac{1}{2}\dot{M}s-\gamma\tanh(s)\end{pmatrix} \quad (25)$$

Where $\Lambda^{-1}$ always exists.

## 4. SIMULATION RESULTS

To evaluate the performance of the proposed IPBSMC scheme for trajectory tracking of the Quanser Aero 2 helicopter platform, sinusoidal reference signals are employed as desired trajectories. A permanent band-limited white Gaussian noise is introduced as a non-vanishing matched disturbance. Two cases are considered with and without disturbances. The amplitude of the disturbance signal is 10% of the control signal. Simulation results are illustrated in Figures 2 to 6.

### A. Undisturbed System Performance

Under undisturbed conditions, the IPBSMC controller demonstrates good tracking precision for both pitch and yaw axes (Fig. 2). The system exhibits rapid convergence with settling times of approximately 2 seconds for both channels. Steady-state tracking errors are maintained below ±0.05 rad (±2.9°), representing less than 3% deviation from reference amplitudes.

The corresponding control signals (Fig. 3) reveal smooth voltage profiles with peak amplitudes not exceeding ±5.2 V for pitch and ±6 V for yaw. The absence of high-frequency oscillations confirms the successful mitigation of chattering phenomena, a common limitation in traditional sliding mode implementations. The control effort distribution shows balanced energy consumption between axes, with the integral component contributing to zero steady-state error achievement.

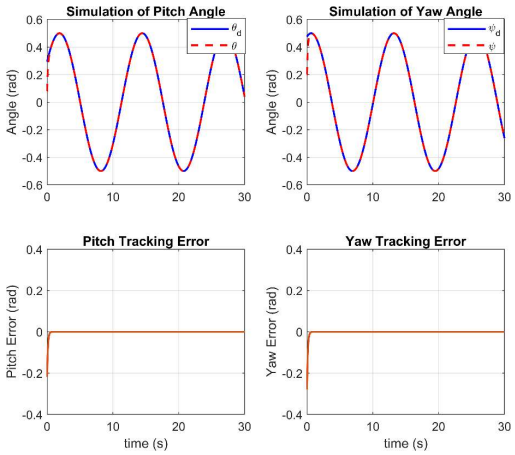


Fig. 2 Undisturbed simulation results of trajectory tracking.

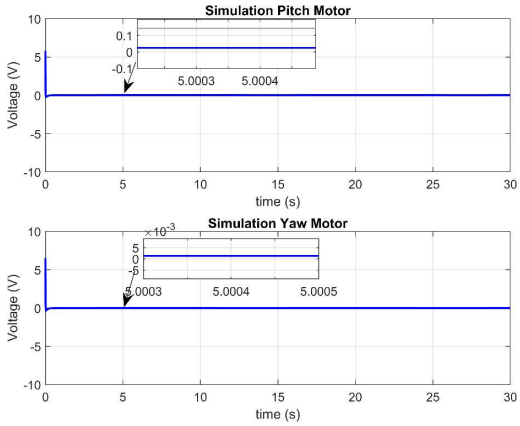


Fig. 3 Undisturbed simulation results of trajectory tracking.

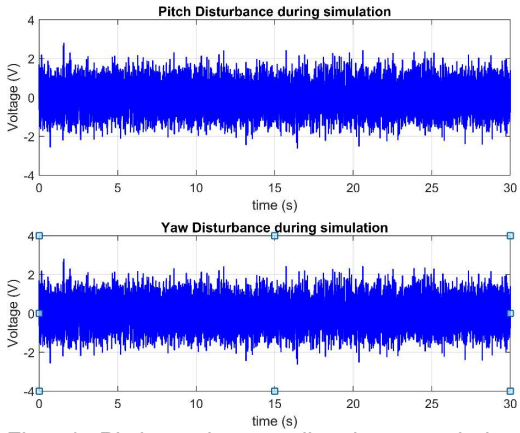


Fig. 4 Pitch and yaw disturbances during simulations.

### B. Disturbed System Robustness

When subjected to band-limited white Gaussian noise disturbances (Fig. 4), the IPBSMC maintains stable trajectory tracking performance with bounded deviations. The maximum angular excursions remain within ±0.6 rad during the most severe disturbance periods.

Transient error analysis (Fig. 5) reveals initial peaks of ±0.35 rad occurring within the first 5 seconds of disturbance application. However, the controller demonstrates rapid recovery, with errors stabilizing to ±0.12 rad within 15 seconds and maintaining a steady-state error of ±0.08 rad. The yaw channel exhibits superior disturbance rejection with lower tracking error compared to pitch, consistent with the platform's dynamic coupling characteristics.

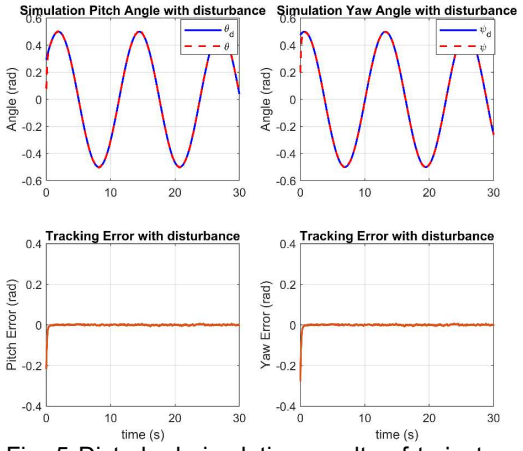


Fig. 5 Disturbed simulation results of trajectory tracking.

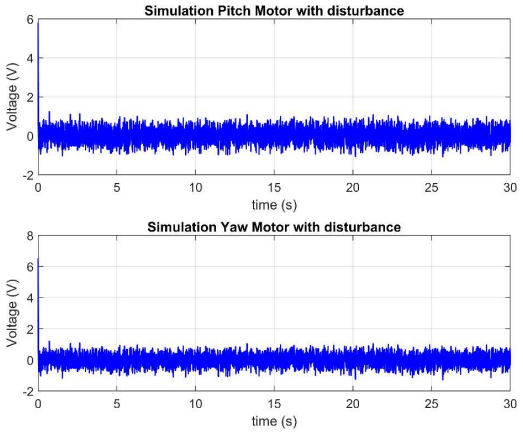


Fig. 6 Disturbed simulation results of pitch and yaw motors.

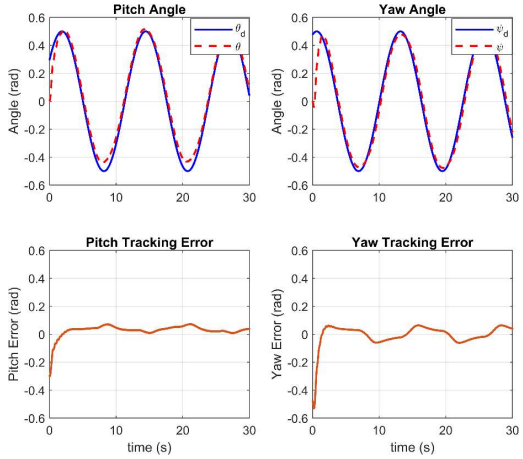


Fig. 7 Undisturbed hardware results of trajectory tracking.

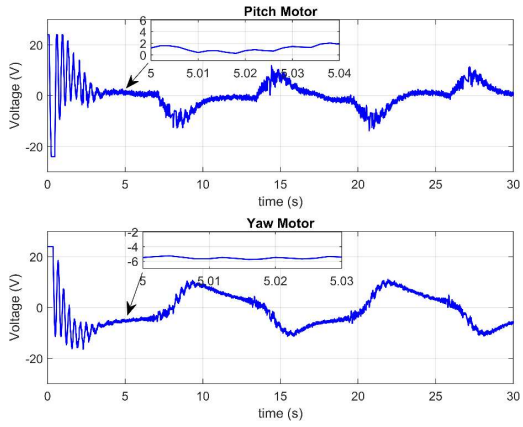


Fig. 8 Undisturbed hardware results of pitch and yaw motors.

The control voltage responses (Fig. 6) show increased activity under disturbances, with peak amplitudes reaching ±7.5 V while remaining well within actuator limits (±24 V). The switching component adapts proportionally to the magnitude of the disturbance, maintaining a consistent ratio between the control effort and the perturbation amplitude. Importantly, the signals retain their smooth characteristics without excessive chattering, validating the passivity-based damping injection mechanism.

## 5. IMPLEMENTATION RESULTS

Experimental validation was conducted on the Quanser Aero 2 platform to demonstrate the real-world applicability of the proposed controller. The hardware implementation preserved the identical test conditions established in simulation to facilitate direct performance correlation and verify the practical effectiveness of the IPBSMC approach under both nominal and noisy operating environments.

### A. Undisturbed Tracking Performance

Real-time experimental results confirm the simulation predictions with remarkable consistency. Under nominal conditions (Fig. 7), the system achieves trajectory tracking with maximum transient deviations of ±0.45 rad, settling to steady-state errors below ±0.1 rad within 4 seconds. The slightly increased settling time compared to the simulation reflects typical modeling uncertainties and hardware limitations inherent in physical implementations. The pitch deviation aligns with the platform's mechanical configuration, where pitch dynamics exhibit higher cross-coupling sensitivity.

Motor voltage profiles (Fig. 8) exhibit smooth characteristics with peak values of ±10.2 V, marginally higher than the simulation due to real-world actuator dynamics. As illustrated in the zoomed sections, the control signals demonstrate excellent regulation without chattering.

### B. Disturbed Case Performance

Under real-time Gaussian disturbances injection (Fig. 9), the system maintains stability with angular deviations constrained to ±0.6 rad. Tracking errors exhibit transient peaks of ±0.4 rad during disturbance injection but recover to ±0.2 rad, confirming the controller's disturbance rejection capability. The yaw axis shows marginally better error suppression (±0.15 rad) compared to pitch (±0.2 rad), likely due to asymmetric system dynamics.

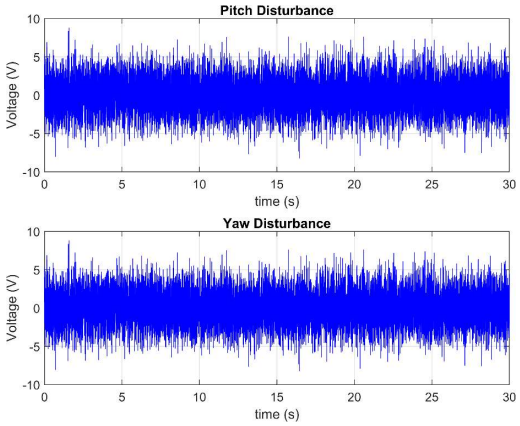


Fig. 9 Disturbances applied to pitch and yaw during hardware implementation.

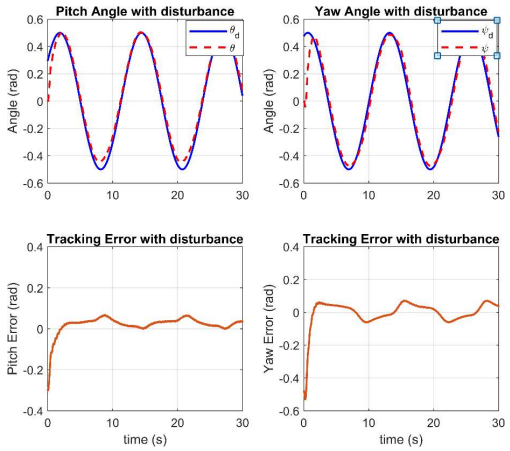


Fig. 10 Disturbed simulation results of trajectory tracking.

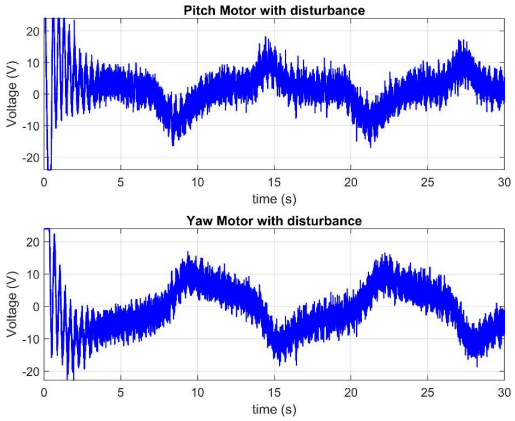


Fig. 11 Disturbed simulation results of trajectory tracking.

Motor voltages (Fig.11) remain within ±15V during disturbances, with pitch control showing higher activity than yaw, reflecting cross-coupling effects. The signals exhibit high-frequency components but avoid destructive chattering, indicating well-tuned switching gains.

## 6. DISCUSSION OF RESULTS

The experimental validation confirms the simulation results with high fidelity, demonstrating the robustness of the proposed IPBSMC approach. The slight discrepancies between simulation and hardware results fall within acceptable ranges for nonlinear control systems. They can be attributed to unmodeled friction, sensor noise, and actuator dynamics not captured in the nominal plant model. The energy-based Lyapunov function provides stability analysis, while the integral sliding surface ensures global robustness from the initial time, eliminating the reaching phase of conventional SMC. Besides, the approach requires accurate knowledge of the inertia matrix for the passivity-based component and good tuning of parameters for applicability to systems with significant parameter uncertainties or under more severe perturbations.

## 7. CONCLUSION

This study successfully demonstrates the effectiveness of integrating passivity-based control with integral sliding mode control for robust trajectory tracking in helicopter-type UAV systems. This framework provides explicit stability guarantees through the passivity-based Lyapunov function while ensuring global robustness via the integral

sliding surface. The comprehensive simulation and experimental validation on the Quanser Aero 2 platform confirm the practical viability of the proposed approach. The results show good trajectory tracking (±0.2 rad steady-state error under non-vanishing Gaussian noise), bounded control effort, and effective noise suppression. Future research should focus on adaptive parameter estimation for systems with uncertain dynamics and multi-objective optimization frameworks for systematic parameter tuning.

### *References*


[1] S. I. Abdelmaksoud, M. Mailah, and A. M. Abdallah, "Control strategies and novel techniques for autonomous rotorcraft unmanned aerial vehicles: A review," IEEE Access, vol. 8, pp. 195142-195169, 2020. doi: 10.1109/ACCESS.2020.3031326

[2] G. Albeaino, M. Gheisari, and B. W. Franz, "A systematic review of unmanned aerial vehicle application areas and technologies in the AEC domain," Journal of information technology in construction, vol. 24, 2019. https://www.itcon.org/2019/20.

[3] A. L'afflitto, R. B. Anderson, and K. Mohammadi, "An introduction to nonlinear robust control for unmanned quadrotor aircraft: How to design control algorithms for quadrotors using sliding mode control and adaptive control techniques [focus on education]," IEEE Control Systems Magazine, vol. 38, no. 3, pp. 102-121, 2018. doi: 10.1109/MCS.2018.2810559.

[4] Quanser. "Aero 2 : Reconfigurable dual-rotor aerospace experiment for controls education and research." (accessed 03/07/2025.

[5] R. Fellag and M. Belhocine, "2-DOF Helicopter Control Via State Feedback and Full/Reduced-Order Observers," in 2024 2nd International Conference on Electrical Engineering and Automatic Control (ICEEAC), 2024: IEEE, pp. 1-6. doi: 10.1109/ICEEAC61226.2024.10576208.

[6] L. B. Prasad, B. Tyagi, and H. O. Gupta, "Optimal control of nonlinear inverted pendulum system using PID controller and LQR: performance analysis without and with disturbance input," International Journal of Automation and Computing, vol. 11, pp. 661-670, 2014. https://doi.org/10.1007/s11633-014-0818-1.

[7] V. I. Utkin, Sliding modes in control and optimization. Springer Science & Business Media, 2013 https://doi.org/10.1007/978-3-642-84379-2

[8] Z. Wang and T. Zhao, "Based on robust sliding mode and linear active disturbance rejection control for attitude of quadrotor load UAV," Nonlinear Dynamics, vol. 108, no. 4, pp. 3485-3503, 2022. https://doi.org/10.1007/s11071-022-07349-y

[9] A. Levant, "Sliding order and sliding accuracy in sliding mode control," International journal of control, vol. 58, no. 6, pp. 1247-1263, 1993. https://doi.org/10.1080/00207179308923053

[10] A. Levant, "Higher-order sliding modes, differentiation and output-feedback control," International journal of Control, vol. 76, no. 9-10, pp. 924-941, 2003. https://doi.org/10.1080/0020717031000099029

[11] V. Utkin and J. Shi, "Integral sliding mode in systems operating under uncertainty conditions," in Proceedings of 35th IEEE conference on decision and control, 1996, vol. 4: IEEE, pp. 4591-4596. doi: 10.1109/CDC.1996.577594.

[12] Y. Pan, C. Yang, L. Pan, and H. Yu, "Integral sliding mode control: performance, modification, and improvement," IEEE Transactions on Industrial Informatics, vol. 14, no. 7, pp. 3087-3096, 2017. doi: 10.1109/TII.2017.2761389.

[13] H. K. Khalil, Nonlinear Systems. Prentice Hall, 2002. https://books.google.dz/books?id=t_d1QgAACAAJ,

[14] I. Fantoni and R. Lozano, Non-linear control for underactuated mechanical systems. Springer Science & Business Media, 2012. https://doi.org/10.1007/978-1-4471-0177-2

[15] R. Ortega, A. Donaire, and J. G. Romero, "Passivity-Based Control of Mechanical Systems," in Feedback Stabilization of Controlled Dynamical Systems: In Honor of Laurent Praly, N. Petit Ed. Cham: Springer International Publishing, 2017, pp. 167-199. https://doi.org/10.1007/978-3-319-51298-3_7

[16] R. Fellag. M. Belhocine. F. Demim. M. Hamel, "Robust Trajectory Tracking of a 2-DOF Helicopter Using Passivity-Based Sliding Mode Control," presented at the National conference on computational engineering, artificial intelligence and smart systems nc2eais2 2024 10-12 December 2024; , Tamanrasset, Algeria;, 2024. [Online]. Available: http://dlibrary.univ-boumerdes.dz:8080/handle/123456789/15097.

[17] F. Li, C. Du, C. Yang, and W. Gui, "Passivity-based asynchronous sliding mode control for delayed singular Markovian jump systems," IEEE Transactions on Automatic Control, vol. 63, no. 8, pp. 2715-2721, 2017. doi: 10.1109/TAC.2017.2776747

[18] C. Ha, Z. Zuo, F. B. Choi, and D. Lee, "Passivity-based adaptive backstepping control of quadrotor-type UAVs," Robotics and Autonomous Systems, vol. 62, no. 9, pp. 1305-1315, 2014. https://doi.org/10.1016/j.robot.2014.03.019